Cationic vacancies and anomalous spectral-weight transfer in $Ti_{1-x}Ta_xO_2$ thin films studied via polarization-dependent near-edge x-ray absorption fine structure spectroscopy

Dong-Chen Qi,[1,2,3,4] Arkajit Roy Barman,[1,2] Lamjed Debbichi,[5] S. Dhar,[1,6,7] Iman Santoso,[1,3] Teguh Citra Asmara,[1,2] Humair Omer,[1,3] Kesong Yang,[8] Peter Krüger,[5] Andrew T. S Wee,[2] T. Venkatesan,[1,2,6] and Andrivo Rusydi[1,2,3,*]

[1]*NUSNNI-Nanocore, National University of Singapore, 5A Engineering Drive 1, Singapore 117411*

[2]*Department of Physics, National University of Singapore, 2 Science Drive 3, Singapore 117542*

[3]*Singapore Synchrotron Light Source, 5 Research Link, Singapore 117603*

[4]*Institute of Materials Research and Engineering (IMRE), 3 Research Link, Singapore 117602*

[5]*ICB, UMR 6303 CNRS-University of Burgundy, F-21078 Dijon, France*

[6]*Department of Electrical and Computer Engineering, National University of Singapore, 4 Engineering Drive 3, Singapore 117576*

[7]*Department of Physics, Shiv Nadar University, Greater Noida, UP 203207, India*

[8]*Department of Mechanical Engineering and Materials Science, Duke University, Durham, North Carolina 27708, USA*

(Received 16 May 2012; revised manuscript received 1 December 2012; published 3 June 2013)

We report the electronic structures of Ta-doped anatase TiO_2 thin films grown by pulsed laser deposition (PLD) with varying magnetization using a combination of first-principles calculations and near-edge x-ray absorption fine structure (NEXAFS) spectroscopy. The roles of Ta doping and Ti vacancies are clarified, and the observed room-temperature ferromagnetism is attributed to the localized magnetic moments at Ti vacancy sites ferromagnetically ordered by electron charge carriers. O K-edge spectra exhibit significant polarization dependence which is discussed and supported by first-principles calculations in relation to both the crystal symmetry and the formation of defects. In particular, anomalous spectral-weight transfer across the entire O K edge for the ferromagnetic thin film is associated exclusively with the occurrence of Ti vacancies and strong correlation effects, which result in the enhancement of the direct interaction between oxygen sites and of the anisotropy of the e_g-p_σ hybridizations in the out-of-plane component. Our results show that O K-edge NEXAFS spectra can provide reliable experimental probes capable of revealing cationic defects that are intimately related to the ferromagnetism in transition metal oxides.

DOI: 10.1103/PhysRevB.87.245201 PACS number(s): 75.50.Pp, 78.70.Dm, 71.55.−i

I. INTRODUCTION

Introducing ferromagnetism into semiconductors and wide band-gap transition metal oxides through dilute doping represents a promising way to combine optical, nonvolatility, and logic functions in a single spintronic device.[1–6] Conventional dilute magnetic semiconductors (DMS) based on Mn-doped GaAs, although demonstrating the most reproducible ferromagnetism, have Curie temperatures well below room temperature and therefore may not be suitable for making practical devices.[2,6,7] On the other hand, dilute magnetic semiconducting oxides (DMSOs), with Curie temperatures above 300 K and exceptionally large magnetic moments, have attracted intensive research efforts both from the point of fundamental understanding and practical applications.[3,6,8–10] Despite mounting evidence reporting observations of room-temperature ferromagnetism in numerous oxide systems with dopants spanning almost the entire row of transition metal elements, DMSOs based on magnetic impurities are still subject to intense debates due to the lack of consistency and reproducibility, as well as spurious magnetic phenomena resulting from secondary phase formation, unknown impurities, clustering, and/or precipitation of the magnetic impurities in the host oxide matrix.[11,12] In recent years there has been more startling discoveries of room-temperature ferromagnetism in nontransition metal-doped (e.g., ZnO:C,[13] ZnO:Ga,[14] and SrO:N[15]) and undoped (e.g., HfO_2,[16] ZnO,[17] TiO_2[18]) oxide systems which call for a better understanding of the material science of magnetic and nonmagnetic dopants in oxides in general and the role of native defects.

The emergence of ferromagnetism in these oxides also challenges our fundamental understanding of the carrier mediated ferromagnetism based on the p-d Zener model.[3] Consequently, there has been an emerging consensus that defects, either in the form of cationic vacancies (e.g., V_{Zn}, V_{Ti}) or oxygen vacancies (i.e., V_O), play crucial roles in mediating or inducing ferromagnetism in oxide materials.[8] For example, Coey *et al.* proposed a bound magnetic polaron model which relies on the large sized oxygen vacancy orbitals that percolate to mediate ferromagnetic exchange coupling between localized magnetic sites.[19] Very recently, by combining x-ray magnetic circular dichroism (XMCD) technique with sophisticated first-principles calculations, we explicitly showed the indispensable roles of both oxygen vacancies and magnetic impurities in inducing room-temperature ferromagnetism in Cu-doped ZnO thin films.[20] Similar observations have also been reported for transition-metal-doped TiO_2, in which a number of experimental studies and theoretical calculations have all suggested the important role played by oxygen vacancies in the origin of ferromagnetism in these systems.[21–23] It was found that the presence of oxygen vacancies in the vicinity of doped impurities cannot only reduce the energy required to introduce impurities into the host lattice, but also enhance the magnetic moments.[22] In addition to transition metal dopants, Nb and Ta-doped TiO_2 are also subject to intense research efforts in view of their promising applications as transparent electrodes used in optoelectronic devices.[24] Using time-differential perturbed-angular-correlation (TDPAC) spectroscopy, the substitution and hyperfine interactions of highly diluted Ta impurities in rutile TiO_2 has been studied in

 ©2013 American Physical Society

atomic scale.[25,26] A very recent study on Nb and Ta-doped TiO_2 using screened-hybrid-density-functional calculations reveals that the metallic nature of doped anatase TiO_2 is due to the delocalization of electrons introduced by the doping in the conduction band of the parent compound, in clear contrast to the semiconducting rutile TiO_2 in which the donated electrons are localized in neighboring Ti sites.[27]

On the other hand, it was theoretically predicted by Elfimov *et al.* that cationic vacancies in a wide band-gap oxide of CaO can introduce localized magnetic moments with concomitant half-metallicity.[28] The formation of such cationic vacancies in oxides can be greatly facilitated by either hole or electron doping.[29] The first experimental observation of local magnetic moments arising from cationic vacancies was reported by Zhang *et al.*,[30] who observed signatures of the Kondo effect below 100 K in 5% Nb-doped anatase TiO_2 thin films. Very recently we have reported ferromagnetism in 5% Ta-doped TiO_2 thin films where by using various sophisticated and element specific techniques including XMCD and optical magnetic circular dichroism (OMCD), we have convincingly shown the spin polarization in the parent oxide bands, which is key to any intrinsic ferromagnetic semiconductors or oxides.[31] In particular, we have shown that the XMCD signals reside dominantly at the Ti t_{2g} derived states, and by separating the contribution of magnetic moments from Ti and O sites using the XMCD sum rules, the observed ferromagnetism is unambiguously found to be originating from Ti sites, or to be more specific the Ti vacancies.[31] Furthermore, in support with the transport result, the observed ferromagnetism was proposed to arise from the electron carrier-mediated exchange interactions similar to the Ruderman-Kittel-Kasuya-Yosida (RKKY) type that couples the local magnetic moments of the Ti vacancies (V_{Ti}) with the donors electrons from the Ta. In both studies, there is a strong correlation between the increase in the spectral weight of the t_{2g} bands in the Ti $L_{3,2}$-edge near-edge x-ray absorption fine structure (NEXAFS) spectra and the occurrence of local magnetic moments and/or ferromagnetic ordering, implying an increase in V_{Ti}. This is then the basic motivation of our current study. If a V_{Ti} is indeed created then the six oxygen sites surrounding the Ti atoms will most likely experience an enhanced interaction with each other, which may present important spectroscopic signatures at the O K edge. Moreover, the O K edge suffers much less severe self-energy influences and therefore well represents the oxygen $2p$-projected unoccupied density of states in TiO_2 in a first-order approximation.[32]

Here we have applied polarization-dependent NEXAFS spectroscopy as a main probe for the electronic states of the Ta-doped anatase TiO_2 system. To identify spectroscopic features that are exclusively associated with Ti vacancies and ferromagnetism, three representative anatase TiO_2 thin films with prominent c-axis texture are studied and compared, including a nonmagnetic pure TiO_2 thin film ($M^{sat.} < 0.02$ emu/g), a nonmagnetic conducting TiO_2 thin film with 5% Ta doping grown at the substrate temperature of 700 °C ($M^{sat.} < 0.06$ emu/g; denoted NM sample hereafter), and a ferromagnetic conducting TiO_2 thin film with 5% Ta doping grown at the substrate temperature of 600 °C ($M^{sat.} = 4.1$ emu/g, denoted FM sample hereafter). These three samples are our model system and have been well characterized in our previous study.[31] For the sake of reproducibility, we also perform O K-edge NEXAFS spectra for 5% Ta-doped anatase TiO_2 films grown under varying oxygen partial pressure with substrate temperature kept at 700 °C, which shows consistent results. Anomalous spectral-weight transfer at the O K edge which can be associated with the formation of Ti vacancies and a direct fingerprint of strong correlations has been found for the FM sample, pointing to the correlation between Ti vacancy and ferromagnetism.

II. EXPERIMENTAL DETAILS

A. Sample preparation

Anatase Ta-doped TiO_2 epitaxial thin films were deposited on high-quality (001) $LaAlO_3$ substrates by pulse laser deposition (PLD) using a 248-nm Lambda Physik excimer laser with an energy density of 1.8 J/cm^2 and a repetition rate of 5–10 Hz. The PLD targets were made from high-purity (99.999%) Ta_2O_5 and TiO_2 powders that were carefully weighed, mixed, and ground for several hours before being sintered in a furnace at 1000 °C for 20 h. Next, target pellets were made and calcinated at 1100 °C for 24 h. Depositions were performed in a stable oxygen partial pressure of 1×10^{-5} Torr for the growth of all TiO_2 samples unless otherwise specified. The pure TiO_2 film was grown with substrate temperature kept at 700 °C, while two 5% TiO_2:Ta films were grown with substrate temperature of 600 and 700 °C, respectively.

B. Material characterizations

1. *Structural properties*

The crystalline phase of all films was characterized by x-ray diffraction (XRD) using a Bruker D8 x-ray diffractometer. All TiO_2 films were found to be in perfect anatase phase with prominent (001) surface orientation, and no other phases were observed within its detection limit. The crystal quality, the exact Ta concentrations, as well as the substitutionality of Ta at the Ti lattice sites were measured quantitatively using Rutherford backscattering spectrometry (RBS)-ion channeling spectroscopy. RBS showed that most (more than 99%) of the Ta was substitutional in the Ti sites, and the actual Ta concentrations in the films were found to be about 5.5 ± 0.3%. There is no segregation of Ta oxides detected. In order to eliminate the effect of any magnetic impurity artifacts, thorough material characterizations including RBS spectroscopy, proton induced x-ray emission (PIXE), and secondary ion mass spectroscopy (SIMS) were performed on all TiO_2 thin films. Unintended magnetic impurities (e.g., Co, Fe, Ni, Mn, Cr) were found to be negligible with concentration substantially below 0.01%.[31]

2. *Electrical properties and oxygen substoichiometry*

The pure anatase TiO_2 sample displays n-type conductivity with the electron carrier density in the order of 10^{17} to 10^{19} cm^{-3}, suggesting the existence of native oxygen vacancies. However, the TiO_2 films become highly conductive with the electron carrier density in the order of 10^{20} cm^{-3} after 5% Ta doping, and the electrical properties are dominantly modulated by Ta doping.

3. Magnetic properties

Superconducting quantum interference device (SQUID) measurements (Quantum Design) were performed at room temperature to characterize the magnetic properties of TiO_2 samples. Strong room-temperature ferromagnetism with saturation magnetization of 4.1 emu/g and coercivity of about 80 Oe was found for the FM 5% TiO_2:Ta thin film grown at 600 °C. In contrast, saturation magnetization less than 0.1 emu/g was found for the NM 5% TiO_2:Ta thin film grown at 700 °C ($M^{sat.} < 0.06$ emu/g) as well as the pure TiO_2 sample ($M^{sat.} < 0.02$ emu/g). The $LaAlO_3$ substrates treated under similar process conditions only show diamagnetic behavior.

C. NEXAFS measurements

NEXAFS measurements at O K edge were obtained in total electron yield (TEY) acquisition mode by recording sample current as a function of photon energy of incident x rays at the SINS beamline of Singapore Synchrotron Light Source (SSLS) in a ultrahigh vacuum (UHV) chamber with a base pressure of 1×10^{-10} mbar.[33] Linearly polarized x-ray beam with a degree of polarization better than 90% and energy resolution better than 200 meV was employed for the NEXAFS measurements. The incidence angle (θ) of x rays with respect to the sample surface plane was varied by rotating the polar angle of the sample. All NEXAFS spectra were normalized by the incident x-ray intensity (I_0) monitored by a refocusing mirror to eliminate the fluctuation in the incident x-ray intensity. It should be noted that NEXAFS spectroscopy is a surface-sensitive probe with probing depth around 10–100 nm. However, as the ferromagnetism in Ta-TiO_2 had been thoroughly characterized by both bulk-sensitive probes, including SQUID and OMCD, and surface sensitive probe of XMCD (with essentially the same probing depth as that of NEXAFS). The room-temperature ferromagnetism is therefore established as an intrinsic property of a Ta-doped TiO_2 system rather than any surface or interface effect. Consequently, the information accessed by NEXAFS is relevant to revealing the correlation between ferromagnetism and V_{Ti} in the present study.

III. COMPUTATIONAL DETAILS

A. Spin-polarized electronic structures

First-principles calculations within spin-polarized generalized-gradient approximation plus on-site U parameter (GGA + U) were performed to model the electronic structures of TiO_2 samples. A 48-atom supercell consisting of $2 \times 2 \times 1$ repetition of the conventional unit cell of anatase TiO_2 was constructed, in which a Ti atom was either replaced by a Ta atom (corresponding to 6.25% Ta doping concentration) or was removed (corresponding to 6.25% V_{Ti} concentration). To model the electronic structures of TiO_2 with the coexistence of V_{Ti} and Ta (1:1 ratio), a Ta atom was placed at the first nearest neighbor site of a V_{Ti} in the same 48-atom supercell structure. The projector augmented wave (PAW) potentials and the generalized gradient approximation parametrized by Perdew and Wang (PW91) were used to deal with electron-ion interactions and the electron exchange-correlation functional, respectively.[34,35] The cut-off energy of 400 eV and the $2 \times 2 \times 2$ k-point mesh centered at Γ point are used. All the atomic positions were fully relaxed until all components of the residual forces were smaller than 0.025 eV/Å. The density of states was calculated using the tetrahedron method with Blöchl corrections.[36] In our GGA + U calculations, the calculated on-site effective U parameter ($U_{eff} = U$-J) was adopted for Ti $3d$ (5.8 eV) and Ta $5d$ (3.0 eV) electrons.[37] Our spin-polarized GGA + U electronic structure calculations were carried out using the Vienna *ab initio* simulation package (VASP).[38,39]

B. Calculation of O K-edge NEXAFS spectra

The O K-edge spectra were calculated within density functional theory using the Vienna *ab initio* simulation package.[38,39] The energy cutoff was set to 400 eV and the Brillouin zone of the tetragonal cell was sampled with a $8 \times 8 \times 4$ mesh. The O K-edge spectra of TiO_2 are well described by the O $2p$ projected ground state density of states (DOS) because core-hole effects are negligible at this edge.[40] Finite lifetime of the x-ray absorption final state can be accounted for by Lorentzian broadening. Following the prescription of the MXAN code[41] we used a Lorentzian of energy-dependent width $\Gamma(E) = \Gamma_c + A\{0.5 + \arctan[(E - E_s)/b]/\pi\}$. Here Γ_c is the natural width of the O $1s$ hole (0.156 eV) and E_s is the step position which was taken as the plasmon peak of anatase (12.7 eV).[42] The parameters $A = 1$ eV (step height) and $b = 2$ eV have been adjusted to the experiment.

IV. RESULTS AND DISCUSSION

A. The origin of ferromagnetism in Ta-doped TiO_2: A theoretical revisit

In Ref. 31 a surprising room-temperature ferromagnetism in 5% Ta-doped anatase TiO_2 thin films was reported. To unravel the origin of ferromagnetism in this complex oxide system, it is important to understand not only the roles of the constituent atoms (i.e., Ti, O, Ta) and the native defect centers (i.e., V_O, V_{Ti}), but also their interactions. Since the parent TiO_2 compound exhibits no magnetic behavior, the observed ferromagnetism most likely orignates from the defect centers or the incorpoated Ta atoms, or through the interactions of both. Using first-principles calcluations, Peng *et al.* showed that an oxygen vacancy does not produce a magnetic moment and the DOS remains spin unpolarized for a oxygen-deficent anatase TiO_2 system.[43] This is consistent with our experimental findings that the pure TiO_2 sample, which is known to contain oxygen vacancies based on its moderate n-type conducitivity, is not ferromagnetic. Ta doping, on the other hand, results in spin-polarized DOS with the magnetic moments (1 μ_B per Ta) predominantly residing in Ti $3d(t_{2g})$ bands.[31] However, theoretical calculations have predicted them to be coupled antiferromagnetically[44] and the system is nonmagnetic.[27] By using elemental and orbital specific magnetic probes (i.e., XMCD and OMCD), the observed ferromagnetism in Ta-doped TiO_2 is ascribed to the magnetic moments exclusively associated with Ti vacancies (V_{Ti}).[31] Indeed, our DFT calculations for TiO_2 with Ti vacancies (without Ta doping) clearly show spin polarization near the valence band edge which is predominanntly contributed by spin splitting in the oxygen $2p$ bands [(Figs. 1(a) and 1(b)]. This is consistent with previous first-principles calculations

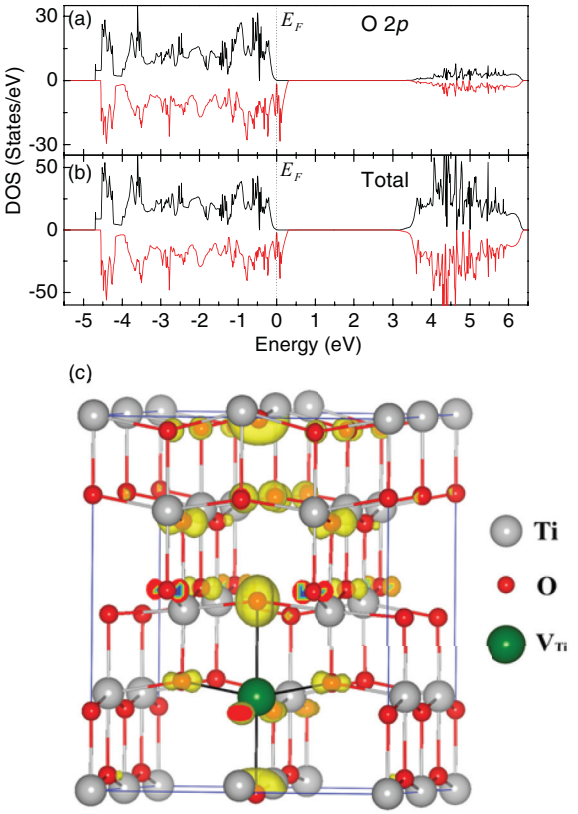

FIG. 1. (Color online) Spin-resolved (a) partial density of states (DOS) for O $2p$ states, (b) total DOS, and (c) calculated spin-density isosurfaces of anatase TiO_2 with V_{Ti}.

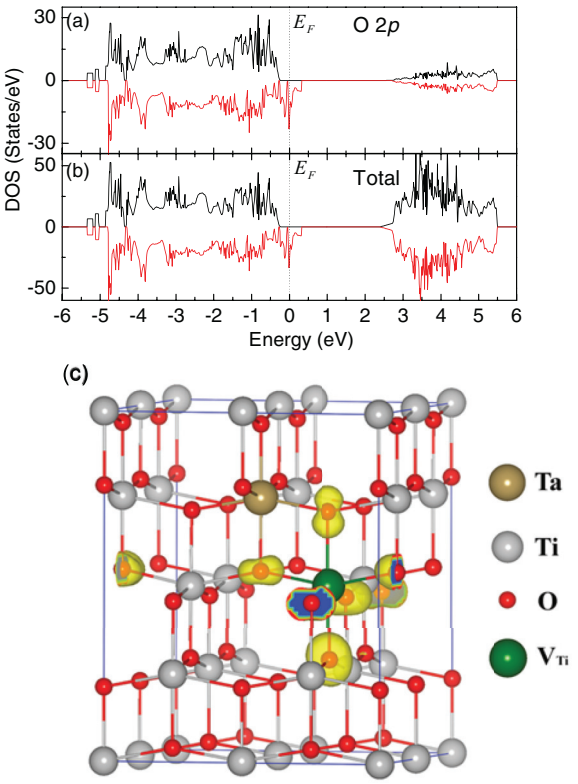

FIG. 2. (Color online) Spin-resolved (a) partial DOS for O $2p$ states, (b) total DOS, and (c) calculated spin-density isosurfaces of anatase Ta-doped TiO_2 with V_{Ti}.

carried out by Peng *et al.*[43] The spin density distribution around the V_{Ti} magnetic center can be visualized by the calculated spin-density isosurfaces in Fig. 1(c), showing that the magnetic moments are mainly distributed on the six adjacent oxygen sites with more weights over the two apical O atoms, and it generates a total magnetic moment of 4.0 μ_B (per V_{Ti}). Furthermore, to evaluate the relative stability of the ferromagnetic (FM) and antiferromagnetic (AFM) alignments between the magnetic moments on the two V_{Ti}, we performed calculations using a 216-atom $3 \times 3 \times 2$ supercell, in which two V_{Ti} are introduced and their distance is about 7.6 Å. The FM state is found to be more stable than the AFM state by 112 meV in total energy. This indicates that the V_{Ti} can potentially be ferromagnetically coupled provided that the V_{Ti} concentration reaches the percolation threshold. This ferromagnetic coupling among V_{Ti} could be facilitated by the presence of Ta doping through the electron carrier-mediated exchange interactions (such as the RKKY-type) even if the vacancy concentration is well below the percolation threshold.

In contrast to the relatively simple scenario of modeling TiO_2 containing only Ta or V_{Ti}, modeling of Ta-doped TiO_2 with the coexistence of V_{Ti} and calculating its magnetic properties are much more challenging. The uncertainty of the vacancy concentration and the relative position between Ta atoms and V_{Ti} greatly increase the calculation complexity. Nevertheless, we can make some general predictions on its magnetic properties based on our current understanding of the roles played by V_{Ti} and Ta doping, respectively. A V_{Ti} carries a magnetic moment of 4 μ_B owing to the four holes it introduces to the surrounding O $2p$ orbitals. Meanwhile, a Ta impurity on average will compensate one hole and reduce the magnetic moment of V_{Ti} to 3 μ_B. Consequently, four Ta impurities will fully compensate the V_{Ti} and eliminate its magnetic moment. However, we need the Ta doping in order to more effectively couple the V_{Ti} magnetic centers via carrier-mediated interactions. Therefore, the ideal ratio between Ta and V_{Ti} should be below 4:1. As an example, we have shown here the calculated spin-polarized DOS [Figs. 2(a) and 2(b)] and the spin density plot [Fig. 2(c)] for a particular TiO_2 supercell in which a Ta atom is at the first-neighbor site of the V_{Ti} (corresponding to 1:1 ratio). As expected, both the electronic structures and the spin density distribution of this system greatly resemble those of the TiO_2 with only V_{Ti}. The spin split still occurs in the valence band edge (composed of O $2p$), and the total magnetic moment is mainly contributed by the oxygen ions around the V_{Ti} center.

B. Polarization-dependent O *K*-edge NEXAFS spectra

Figure 3 shows the polarization-dependent O K-edge NEXAFS spectra for all three samples. The polarization of the incident synchrotron light is changed by varying the incidence angle (θ) of x rays with respect to the sample surface plane. The first two sharp resonances (A and B) with an energy separation around 2.7 eV correspond well to the Ti $3dt_{2g}$-e_g split, and they are ascribed to the excitations into these states

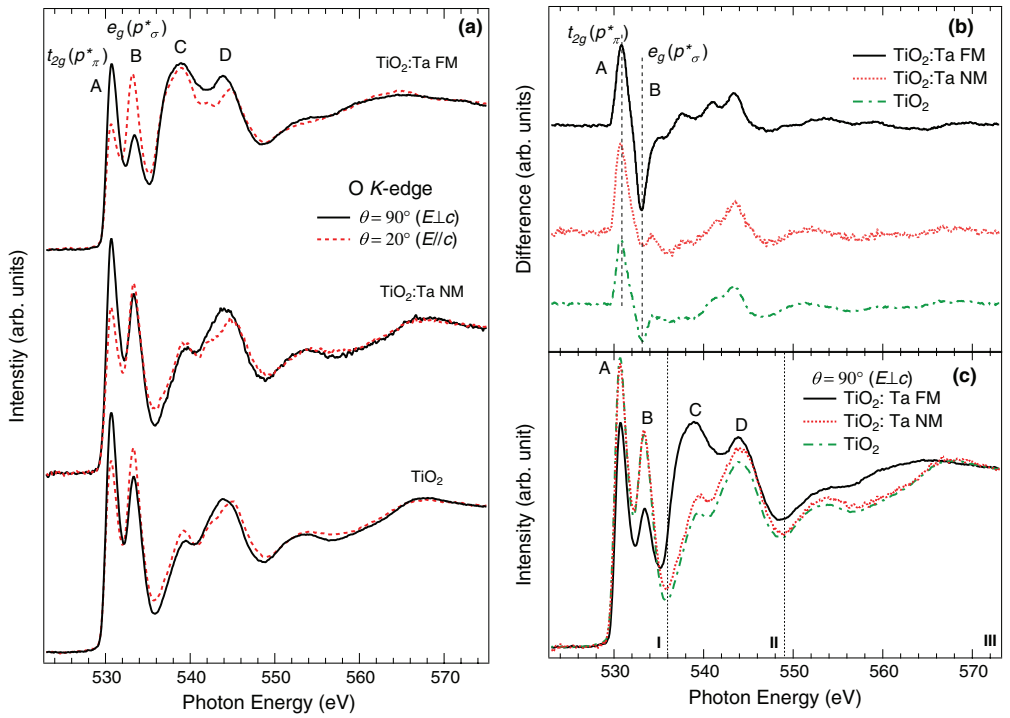

FIG. 3. (Color online) (a) Polarization-dependent NEXAFS spectra at O K edge for different TiO_2 samples. (b) The difference spectra obtained by subtracting the grazing incidence spectra ($\theta = 20^\circ$) from the normal incidence spectra ($\theta = 90^\circ$). (c) Comparison of the normal incidence O K-edges spectra for different TiO_2 samples. The vertical dashed lines separate the integration regions. All spectra are normalized to have the same absorption step height.

containing O $2p$ character due to strong covalent mixing. As shown in Fig. 3(a), peaks A and B exhibit significant variation in intensities as a function of the polarization of light. For all three samples, the intensity of peak A (t_{2g}) is strongest at normal incidence angle ($\theta = 90^\circ$) with the electric field vector $\boldsymbol{E}$ perpendicular to the crystallographic c axis ($\boldsymbol{E} \perp \boldsymbol{c}$), whereas it diminishes with decreasing incidence angle and becomes weakest at the grazing incidence angle ($\theta = 20^\circ$) with $\boldsymbol{E}$ close to the normal of the sample surface ($E \parallel c$). The polarization dependence of peak B (e_g) exhibits an opposite trend, and the FM TiO_2 sample exhibits larger polarization dependence in the intensity of peak B than the other two samples, which is more easily observed in the linear dichroism spectra shown in Fig. 3(b).

The polarization dependence of NEXAFS resonances is known to rely on the relative alignment between the electric vector $\boldsymbol{E}$ of the incident light and the transition dipole matrix element defined by $\langle f|\mathbf{r}|i\rangle$, where $|f\rangle$, $|i\rangle$, and $\boldsymbol{r}$ denote the final state, initial state, and position vector operator, respectively.[45] For K-edge transitions with a $1s$ initial state, the matrix element is determined by the orbital vector of the $2p$ empty final state. In order to understand deeper on the origin of NEXAFS spectra, we perform first-principles calculations on the charge densities of the related empty states. The results, which are shown in Figs. 4(a) and 4(b), clearly reveal that the Ti $3dt_{2g}$ orbitals are weakly π antibonding with the O p_π components in the first unoccupied state (peak A), and the Ti e_g orbitals are strongly σ antibonding with the O p_σ orbitals, which is consistent with earlier assignments.[46] While the O p_π components which are comprised of O $2p_x$ or $2p_y$ orbitals are essentially parallel to the (001) surface plane ($\perp c$), the O p_σ contributions tend to be isotropic, containing both the p_z orbitals in the out-of-plane (apical, $\parallel c$) direction and in-plane p_x or p_y orbitals (equatorial, $\perp c$). However, the out-of-plane p_σ contribution is expected to dominate over the in-plane contribution due to the distortion of the TiO_6 octahedra. Consequently, the observed disparity in the polarization dependence of peaks A and B at O K edge can be qualitatively explained by the directional nature of the O $2p$ final states. Indeed, we are able to reproduce all the major absorption features and their polarization dependence by simulating the O K-edge spectra using first-principles calculations [cf. Fig. 4(e)].

C. Spectral-weight transfer in the O K edge

In addition to the slight difference in the polarization dependence of O K edge, the spectral-weight distributions across the entire absorption edge up to 40 eV are remarkably different for the FM TiO_2 film in comparison with the other two samples. As more clearly shown in Fig. 3(c), while the t_{2g} and e_g components are reduced in intensity for the FM sample, the broad and asymmetric absorption feature labeled C at higher energy exhibits an enormous enhancement. This means that the *spectral weight of* t_{2g} *and* e_g *derived states are transferred to higher energies for the ferromagnetic sample*. Intriguingly, this spectral-weight transfer (or redistribution) is not observed in the NM Ta-doped TiO_2 sample, indicating that this is not a consequence of Ta doping but rather intimately correlated with the observed ferromagnetism.

To better illustrate the spectral-weight transfer, in Fig. 5(a) we display the relative spectral-weight changes for the three

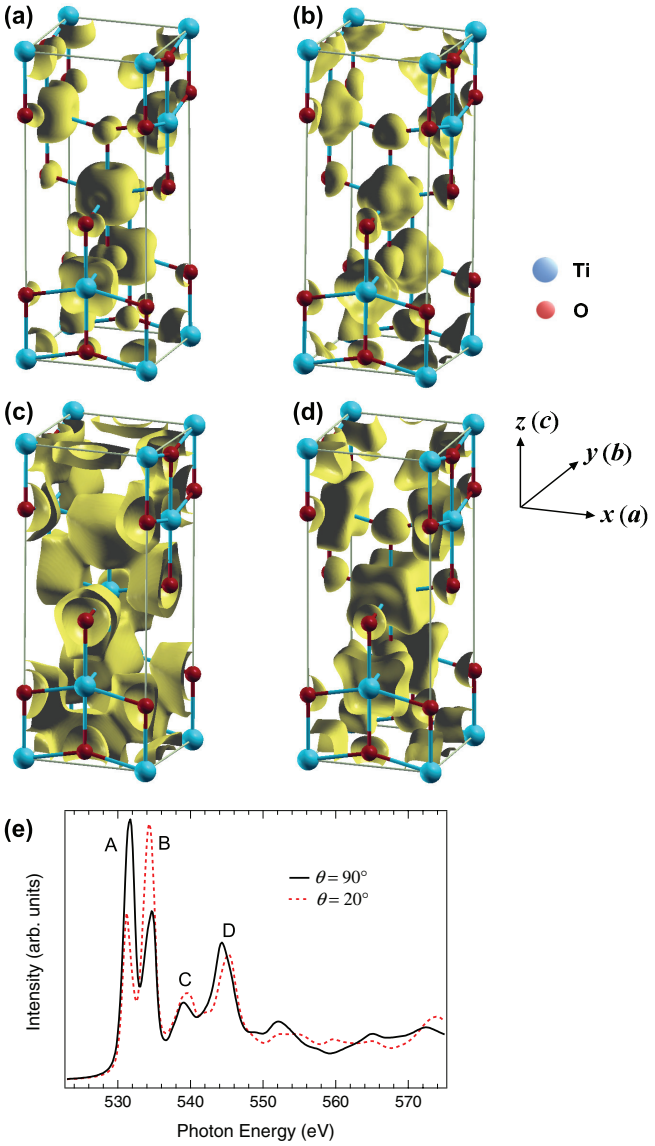

FIG. 4. (Color online) The calculated real-space charge density in the energy intervals corresponding to peak A (a), B (b), C (c), and D (d), respectively, in the O K-edge NEXAFS spectra. (e) The calculated polarization-dependent O K-edge NEXAFS spectra for pure anatase TiO_2. The definition of the incident angle of x rays (θ) is the same as the experiment.

TiO_2 samples with different magnetizations in three representative energy regions covering different absorption features in O K edge [also shown in Fig. 3(c)]. In contrast to the subtle variations in the spectral weights of the NM sample, the spectral weight of region II (536–549 eV) containing the broad features C and D exhibits a sharp increase for the FM sample which is accompanied by a decrease in the spectral weight of region I (523–536 eV) covering the t_{2g} and e_g derived states. The overall spectral weight (W^{total} covering 523 to 573 eV) of the FM sample only sees a slight increase. A schematic diagram illustrating the spectral-weight transfer is shown in Fig. 5(b).

The broad spectral features in O K edge above the first two sharp t_{2g} and e_g resonances can be generally attributed to the antibonding combinations involving O $2p$ and Ti $4sp$ states.

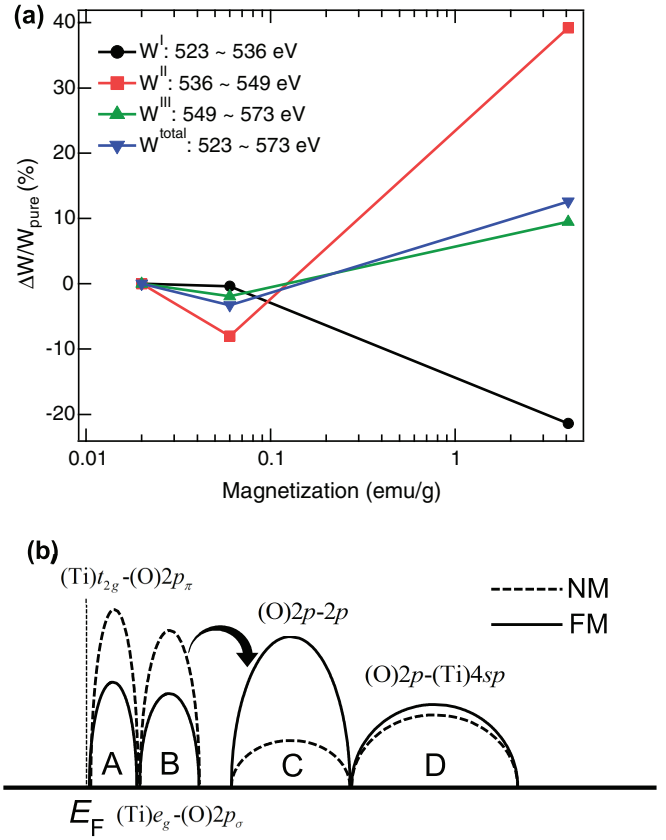

FIG. 5. (Color online) (a) Relative changes of the spectral weight $\Delta W/W_{\text{pure}}$ in different integration regions normalized to the spectral weight of the pure TiO_2 sample in the respective energy ranges as a function of the saturation magnetization (in log scale) of different films. The error bars in the y axis is considerably smaller than the symbols considering the good signal-noise ratio of the O K-edge NEXAFS spectra. (b) Schematic description of the oxygen p-projected unoccupied density of state illustrating the spectral-weight transfer that is associated with the occurrence of ferromagnetism.

To be more specific, the structure C at about 539 eV has been previously attributed to the antibonding σ^* states formed by direct oxygen-oxygen $2p$ interactions, whereas the O $2p$-Ti $4sp$ hybridized states lie at higher energies.[32] This assignment is also confirmed by our first-principles calculations on the O and Ti projected partial density of states with energy range comparable to that of NEXAFS (Fig. 6). As shown in Fig. 6, the first two unoccupied states which correspond to peak A and B in the O K-edge spectra clearly involve strong hybridization between the Ti $3d$ states and the O $2p$ states, whereas peak D involves strong mixing between O $2p$ and Ti $4p$ as well as some Ti $4s$ states. In contrast, peak C contains almost only O $2p$ states with negligible hybridizations with any Ti states. Moreover, as revealed by the calculated real-space charge density contour that corresponds to peak C [cf. Fig. 4(c)], the charges only reside on O sites and the orbital hybridization among adjacent O atoms can be seen. This is in stark contrast to peaks A, B, and D [cf. Figs. 4(a), 4(b), and 4(d)], for which the charges locate on both Ti (dominantly) and O sites. Considering a TiO_6 octahedra, the removal of the Ti atom (by forming a V_{Ti}) at the center of the octahedra would naturally

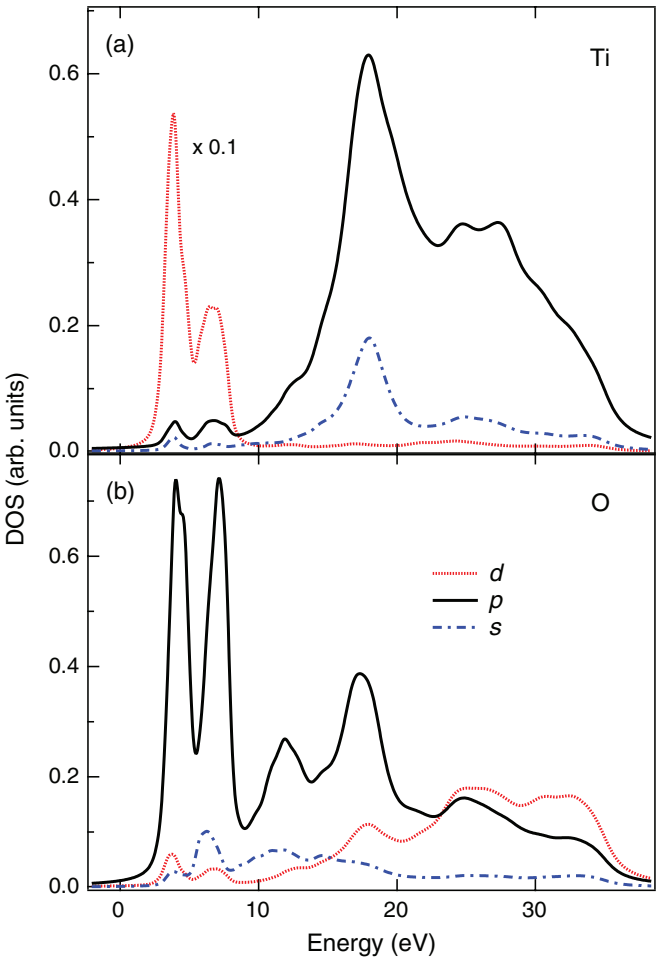

FIG. 6. (Color online) Partial DOS projected onto individual orbitals of (a) Ti and (b) O sites for pure anatase TiO_2.

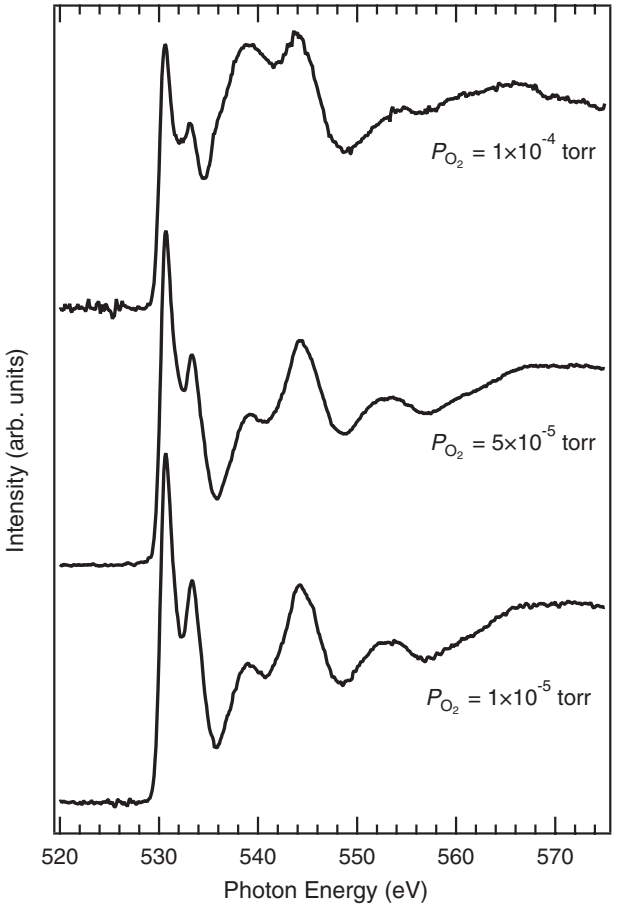

FIG. 7. (Color online) O K-edge NEXAFS spectra for 5% Ta-doped anatase TiO_2 films grown under varying oxygen partial pressure with substrate temperature kept at 700 °C.

enhance the direct orbital overlap between the three pairs of oxygen atoms with their p orbital lobes directed towards the central vacancy site (p_σ), while at the same time eliminate the orbital mixing between the O $2p$ and the Ti $3d$-derived t_{2g} and e_g bands. In addition, it is theoretically predicted that Ti vacancies are prone to pair and form Ti divacancy sites with higher stability.[43] With the removal of two neighboring Ti atoms, the two O atoms that were originally bonded with both Ti atoms relax and form an O_2 dimer in the center of the divacancy.[43] The σ^* resonances associated with an O_2 dimer are known to reside in the region around 540 eV which coincides with the observed C structure in TiO_2.[47] The formation of V_{Ti} is therefore fully consistent with the experimental observation on the spectral-weight transfer from the t_{2g} and e_g derived states to the C state for the FM sample, indicating the intimate correlation between ferromagnetism and Ti vacancies in the Ta-doped TiO_2 samples. Similar spectral-weight transfer has also been observed for a separate set of TiO_2 samples for which the oxygen partial pressure during film growth was increased from 1×10^{-5} to 1×10^{-4} Torr (Fig. 7). It is known that growing oxide films under oxygen rich condition is able to promote the occurrence of cationic vacancies,[30,48] so the characteristic spectral-weight transfer at O K edge is again correlated with the formation of V_{Ti}.

The formation of V_{Ti} not only disrupts the electronic states of the nearest oxygen neighbors but is also expected to influence adjacent TiO_6 octahedra, for example through geometrical relaxations of the surrounding O atoms.[43] This might explain the enhanced polarization dependence for the e_g resonance in the O K-edge spectra for the FM sample [Figs. 3(a) and 3(b)]. We speculate that the geometrical relaxation that follows the creation of V_{Ti} may lead to further distortion of the adjacent TiO_6 octahedra, strengthening the out-of-plane ($\| c$) components of the p_σ-e_g antibonding orbitals while weakening the in-plane components ($\perp c$).

The anomalous spectral-weight enhancement of the high-lying state C accompanied by diminishing t_{2g}-e_g derived states at O K edge, therefore, represents a spectroscopic signature for the formation of V_{Ti} and surprisingly strong correlation effects in this system. The phenomenon of anomalous large spectral-weight transfer in a very broad energy range (20 eV and above) is analogous to our recent observation of large spectral-weight transfer in the optical conductivity for $La_{0.7}Ca_{0.3}MnO_3$ from paramagnetic insulating to the ferromagnetic metallic state.[49] As shown by previous theoretical studies, large spectral-weight transfer is a direct fingerprint of strong correlations.[50–54] Our result thus suggests that strong correlations may play a crucial role in the ferromagnetic Ta-TiO_2 films and this may provide important new insights to the theoretical modeling of the

Ta-TiO_2 system. Furthermore, given the high free electron carrier density of about 7.6×10^{20} cm^{-3} provided by the 5% Ta doping at optimal condition,[31] the large localized magnetic moments associated with Ti vacancies are most likely to be coupled by itinerant electron-mediated exchange interactions (such as the RKKY-type), resulting in the observed ferromagnetism. It is thus understandable that the magnetic properties of the Ta-TiO_2 thin films depend very sensitively on the PLD growth conditions,[55] as the optimum number of both V_{Ti} and electron carriers (provided by Ta doping) is crucial to achieve ferromagnetism. This also explains why the other 5% Ta-doped sample with comparable free electron carrier density (8.75×10^{20} cm^{-3}) but deposited at higher substrate temperature of 700 °C appears to be nonmagnetic, as the elevated growth temperature helps to anneal out defect centers and improve the crystallinity of the thin films as suggested by the RBS ion channeling studies.[55]

V. CONCLUSIONS

In conclusion, we have studied the electronic states and magnetic properties of Ta-doped anatase TiO_2 thin films using first-principles calculations and polarization-dependent NEXAFS spectroscopy. The ferromagnetism in the 5% Ta-doped TiO_2 is attributed to the magnetic moments associated with Ti vacancies, and the ferromagnetic coupling is most probably realized through the electron carrier-mediated exchange interactions (such as the RKKY-type) facilitated by Ta doping. Significant spectral-weight transfer across the O K edge from the t_{2g} and e_g derived states to the antibonding states formed by direct oxygen-oxygen $2p$ interactions is found for the ferromagnetic 5% Ta-TiO_2 film, and it represents the spectroscopic signature for the formation of Ti vacancies and suggests the importance of strong correlations. The observed correlation between ferromagnetism and Ti vacancy helps to clarify the origin of ferromagnetism in Ta-doped TiO_2 thin films. Identification of cationic vacancy through the characteristic spectral-weight transfer in the O K edge could be applied to other transition metal oxides as well, and it provides a valuable gauge to facilitate the realization of controlled ferromagnetism in oxides through defect engineering.

ACKNOWLEDGMENTS

This work is supported by Singapore National Research Foundation under its Competitive Research Funding (NRF-CRP 8-2011-06 and NRF2008NRF-CRP002–024), MOE-AcRF-Tier-2, NUS-YIA, and FRC.

*phyandri@nus.edu.sg

[1] K. Ando, Science **312**, 1883 (2006).
[2] H. Ohno, Science **281**, 951 (1998).
[3] T. Dietl, H. Ohno, F. Matsukura, J. Cibert, and D. Ferrand, Science **287**, 1019 (2000).
[4] I. Žutić, J. Fabian, and S. Das Sarma, Rev. Mod. Phys. **76**, 323 (2004).
[5] S. A. Wolf, D. D. Awschalom, R. A. Buhrman, J. M. Daughton, S. von Molnár, M. L. Roukes, A. Y. Chtchelkanova, and D. M. Treger, Science **294**, 1488 (2001).
[6] T. Dietl, Nat. Mater. **9**, 965 (2010).
[7] A. Korbecka and J. A. Majewski, Low Temp. Phys. **35**, 53 (2009).
[8] S. B. Ogale, Adv. Mater. **22**, 3125 (2010).
[9] J. Rebecca, G. Priya, and A. S. Nicola, J. Phys.: Condens. Matter **17**, R657 (2005).
[10] Y. Matsumoto *et al.*, Science **291**, 854 (2001).
[11] D. W. Abraham, M. M. Frank, and S. Guha, Appl. Phys. Lett. **87**, 252502 (2005).
[12] J. Coey and S. Chambers, MRS Bull. **33**, 1053 (2008).
[13] H. Pan *et al.*, Phys. Rev. Lett. **99**, 127201 (2007).
[14] V. Bhosle and J. Narayan, Appl. Phys. Lett. **93**, 021912 (2008).
[15] I. S. Elfimov, A. Rusydi, S. I. Csiszar, Z. Hu, H. H. Hsieh, H. J. Lin, C. T. Chen, R. Liang, and G. A. Sawatzky, Phys. Rev. Lett. **98**, 137202 (2007).
[16] M. Venkatesan, C. B. Fitzgerald, and J. M. D. Coey, Nature (London) **430**, 630 (2004).
[17] Q. Xu *et al.*, Appl. Phys. Lett. **92**, 082508 (2008).
[18] N. H. Hong, J. Sakai, N. Poirot, and V. Brizé, Phys. Rev. B **73**, 132404 (2006).
[19] J. M. D. Coey, M. Venkatesan, and C. B. Fitzgerald, Nat. Mater. **4**, 173 (2005).
[20] T. S. Herng *et al.*, Phys. Rev. Lett. **105**, 207201 (2010).
[21] S. Duhalde *et al.*, Phys. Rev. B **72**, 161313 (2005).
[22] L. A. Errico, M. Rentería, and M. Weissmann, Phys. Rev. B **72**, 184425 (2005).
[23] M. Weissmann and L. A. Errico, Phys. B **398**, 179 (2007).
[24] T. Hitosugi, N. Yamada, S. Nakao, Y. Hirose, and T. Hasegawa, Phys. Status Solidi A **207**, 1529 (2010).
[25] J. M. Adams and G. L. Catchen, Phys. Rev. B **50**, 1264 (1994).
[26] G. N. Darriba, L. A. Errico, P. D. Eversheim, G. Fabricius, and M. Rentería, Phys. Rev. B **79**, 115213 (2009).
[27] T. Yamamoto and T. Ohno, Phys. Rev. B **85**, 033104 (2012).
[28] I. S. Elfimov, S. Yunoki, and G. A. Sawatzky, Phys. Rev. Lett. **89**, 216403 (2002).
[29] J. Osorio-Guillén, S. Lany, and A. Zunger, Phys. Rev. Lett. **100**, 036601 (2008).
[30] S. Zhang *et al.*, Adv. Mater. **21**, 2282 (2009).
[31] A. Rusydi *et al.*, Philos. Trans. R. Soc. A **370**, 4927 (2012).
[32] F. M. F. de Groot, J. Faber, J. J. M. Michiels, M. T. Czyżyk, M. Abbate, and J. C. Fuggle, Phys. Rev. B **48**, 2074 (1993).
[33] X. J. Yu, O. Wilhelmi, H. O. Moser, S. V. Vidyaraj, X. Y. Gao, A. T. S. Wee, T. Nyunt, H. J. Qian, and H. W. Zheng, J. Electron. Spectrosc. Relat. Phenom. **144**, 1031 (2005).
[34] P. E. Blöchl, Phys. Rev. B **50**, 17953 (1994).
[35] J. P. Perdew and Y. Wang, Phys. Rev. B **45**, 13244 (1992).
[36] P. E. Blöchl, O. Jepsen, and O. K. Andersen, Phys. Rev. B **49**, 16223 (1994).
[37] V. I. Anisimov, J. Zaanen, and O. K. Andersen, Phys. Rev. B **44**, 943 (1991).
[38] G. Kresse and J. Furthmuller, Comput. Mater. Sci. **6**, 15 (1996).
[39] G. Kresse and J. Furthmuller, Phys. Rev. B **54**, 11169 (1996).

[40]Z. Y. Wu, G. Ouvrard, P. Gressier, and C. R. Natoli, Phys. Rev. B **55**, 10382 (1997).
[41]M. Benfatto, S. D. Longa, and P. D. Angelo, Phys. Scr. **2005**, 28 (2005).
[42]S.-D. Mo and W. Y. Ching, Phys. Rev. B **51**, 13023 (1995).
[43]H. Peng, J. Li, S.-S. Li, and J.-B. Xia, Phys. Rev. B **79**, 092411 (2009).
[44]K. Yang, Y. Dai, B. Huang, and Y. Feng, Phys. Rev. B **81**, 033202 (2010).
[45]J. Stöhr, *NEXAFS Spectroscopy* (Springer, Berlin, 1992).
[46]R. Asahi, Y. Taga, W. Mannstadt, and A. J. Freeman, Phys. Rev. B **61**, 7459 (2000).
[47]W. Wurth, J. Stöhr, P. Feulner, X. Pan, K. R. Bauchspiess, Y. Baba, E. Hudel, G. Rocker, and D. Menzel, Phys. Rev. Lett. **65**, 2426 (1990).
[48]K. Kowalski, M. Ijjaali, T. Bak, B. Dupre, J. Nowotny, M. Rekas, and C. C. Sorrell, J. Phys. Chem. Solids **62**, 537 (2001).
[49]A. Rusydi *et al.*, Phys. Rev. B **78**, 125110 (2008).
[50]M. A. Majidi, H. Su, Y. P. Feng, M. Rübhausen, and A. Rusydi, Phys. Rev. B **84**, 075136 (2011).
[51]H. Eskes, M. B. J. Meinders, and G. A. Sawatzky, Phys. Rev. Lett. **67**, 1035 (1991).
[52]Y. Ohta, K. Tsutsui, W. Koshibae, T. Shimozato, and S. Maekawa, Phys. Rev. B **46**, 14022 (1992).
[53]M. B. J. Meinders, H. Eskes, and G. A. Sawatzky, Phys. Rev. B **48**, 3916 (1993).
[54]P. Phillips, Rev. Mod. Phys. **82**, 1719 (2010).
[55]A. R. Barman, A. Annadi, K. Gopinadhan, W. M. Lu, Ariando, S. Dhar, and T. Venkatesan, AIP Adv. **2**, 012148 (2012).